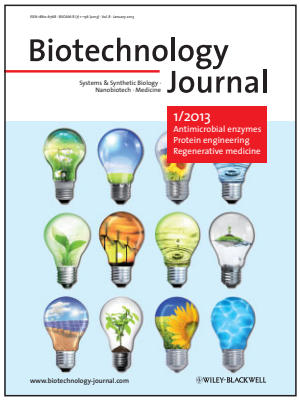

Cover illustration

Special issue *Methods and Advances*

Progress in biotechnology research relies heavily on innovative ideas and approaches. Every year, *Biotechnology Journal* publishes a "Methods and Advances" Special Issue, which covers the latest cutting-edge research and breakthrough technologies. For this issue's cover, we chose a design featuring 12 light bulbs, representing the 12 months of the year, each with state-of- the-art research. Image credits: ©Kletr, ©Natis, ©Sarunyu_foto, ©Scanrail, ©Sergey Niven, ©Thaut Images, ©Yahia LOUKKAL, all from Fotolia.com.

Biotechnology Journal – list of articles published in the January 2013 issue.

Research Article

Nanoscale structure of type I collagen fibrils: Quantitative measurement of D-spacing

Blake Erickson[1,2,], Ming Fang[2,3,*], Joseph M. Wallace[4], Bradford G. Orr[2,5,6], Clifford M. Les[7] and Mark M. Banaszak Holl[1,2,3,5]*

[1] Program in Biophysics, University of Michigan, Ann Arbor, MI, USA
[2] Michigan Nanotechnology Institute for Medicine and Biological Sciences, Ann Arbor, MI, USA
[3] Department of Chemistry, University of Michigan, Ann Arbor, MI, USA
[4] Biomedical Engineering, Indiana University-Purdue University, Indianapolis, IN, USA
[5] Program in Applied Physics, University of Michigan, Ann Arbor, MI, USA
[6] Department of Physics, University of Michigan, Ann Arbor, MI, USA
[7] Bone and Joint Center, Henry Ford Hospital, Detroit, MI, USA

This article details a quantitative method to measure the D-periodic spacing of type I collagen fibrils using atomic force microscopy coupled with analysis using a two-dimensional fast fourier transform approach. Instrument calibration, data sampling and data analysis are discussed and comparisons of the data to the complementary methods of electron microscopy and X-ray scattering are made. Examples of the application of this new approach to the analysis of type I collagen morphology in disease models of estrogen depletion and osteogenesis imperfecta (OI) are provided. We demonstrate that it is the D-spacing distribution, not the D-spacing mean, that showed statistically significant differences in estrogen depletion associated with early stage osteoporosis and OI. The ability to quantitatively characterize nanoscale morphological features of type I collagen fibrils will provide important structural information regarding type I collagen in many research areas, including tissue aging and disease, tissue engineering, and gene knockout studies. Furthermore, we also envision potential clinical applications including evaluation of tissue collagen integrity under the impact of diseases or drug treatments.

Received	27 APR 2012
Revised	23 AUG 2012
Accepted	26 SEP 2012
Accepted article online	02 OCT 2012

Supporting information available online

Keywords: Collagen fibril · D-spacing · 2D fast fourier transform · Atomic force microscopy

Correspondence: Dr. Mark M. Banaszak Holl, Department of Chemistry, University of Michigan, 930 N. University Ave., Ann Arbor, MI 48109-1055, USA
E-mail: mbanasza@umich.edu

Additional correspondence: Prof. Joseph M. Wallace, Department of Biomedical Engineering, 723 W. Michigan SL220D, Indiana University-Purdue University Indianapolis, Indianapolis, IN 46202, USA
E-mail: jmwalla@iupui.edu
Prof. Bradford G. Orr, Department of Physics, 450 Church Street, University of Michigan, Ann Arbor, MI 48109, USA
E-mail: orr@umich.edu

Abbreviations: **2D**, two-dimensional; **AFM**, atomic force microscopy; **CDF**, cumulative distribution function; **ECM**, extracellular matrix; **FFT**, fast fourier transform; **K-S**, Kolmogorov-Smirnov; **OI**, osteogenesis imperfecta; **OVX**, ovariectomized; **SD**, standard deviation; **SEM**, scanning electron microscopy

1 Introduction

Collagens are the most abundant family of structural proteins in animals [1, 2]. These proteins are based on trimeric polypeptide chains, each of which includes a repeating Gly-X-Y triplet region where X and Y are often proline and hydroxyproline. A major class of collagen comprises the fibril-forming types (types I, II, III, V, and XI), which have an approximately 300-nm-long, uninterrupted triple helix [3]. Type I collagen accounts for 70% of all collagens, and it is found throughout the body in the extracellular matrices (ECMs) of teeth, bones, tendons, skin, arterial walls and cornea [4].

* These authors contributed equally to this manuscript.

At the nanoscale, the most prominent feature of type I collagen fibrils is the ~67-nm axial D-periodic spacing. This feature was observed by X-ray diffraction [5] and imaged by transmission electron microscopy as early as 1942 by Schmitt et al. [6]. In 1963, the first model of the fibrillar structure was developed by Hodge and Petruska [7]. They proposed that molecules within a fibril are arranged in a staggered parallel alignment, resulting in "gap" and "overlap" regions [7]. Since this original description, X-ray diffraction [8–11] and electron microscopy [12–14] studies have supported a singular spacing of 67 nm. More detailed models of fibrillar structure have been elucidated by the effort of many researchers, including Miller, Brodsky, Hulmes, and Orgel, to name a few [9, 15–21]. We now know that a fibril is composed of five-stranded microfibrils that are super-twisted in the axial direction [15] and quasi-hexagonally packed in the equatorial plane [16]. An atomistic scale-up simulation based on the state-of-the-art fibril model has elegantly shown the bottom-up design of a collagen fibril resulting in the D-periodicity [22]. Yet all such models are built upon this single valued 67 nm periodicity. Despite this commonly held view of a singular spacing, the hierarchical complexity of the collagen fibril itself, the variety of tissues into which these fibrils are incorporated, and the potential for morphological variation with damage and disease suggests that a single-spacing value for all fibrils is unlikely. Recently, a quantitative approach to measuring this feature allowed the discovery of a distribution of D-periodic spacings ranging from ~60 to 73 nm in normal bone, dentin, skin, and tendon tissue [23]. This distribution changes as a function of estrogen depletion [24, 25] and osteogenesis imperfecta (OI) [26]. This new approach to understanding nanoscale collagen morphology is applicable to understanding the structure of collagen in a wide variety of tissues and ECM-linked diseases.

Quantitative analysis of morphological features in type I collagen-based tissues is imperative to the understanding of normal tissue architecture [23]. This understanding is requisite for interpretation of any alterations caused by damage and disease. These methods may also serve as techniques for disease diagnosis in collagen-based tissues [24–26]. Here we provide important experimental methodology for the application of atomic force microscopy (AFM) to the quantitative analysis of type I collagen D-spacing values. This includes approaches for instrument calibration, data sampling and analysis, and the comparison of D-spacing values obtained with this method to complementary approaches including electron microscopy [12] and X-ray scattering [27]. The experimental approaches should prove useful for quantifying the changes in collagen structure for a wide range of diseases related to the ECM.

2 Materials and methods

2.1 Animals

Five-year-old Columbia-Rambouillet cross sheep were anesthetized and ovariectomized (OVX) or subjected to a sham surgery (Colorado State University, ACUC # 03-010A-02). After 2 years, the ewes were killed with an intravenous overdose of a barbiturate, and skin samples from the dorsal thoracolumbar region were used as previously described [28].

2.2 AFM calibration

Calibration of the Agilent 5500 AFM large scanner (80 μm scan range) was carried out with a 100 nm × 100 nm calibration standard (Nanosensors, Switzerland), using contact mode and SNL-10 AFM probes (nominal tip radius 2 nm, force constant 0.25 N/m. Bruker AFM probes, CA, USA). The scan size was set at 3.5 μm (35 × 35 pitches) with 512 × 512 pixels and a scan rate of 2 lines/s. The absolute error of the calibration standard was verified by scanning electron microscopy (SEM) imaging to be less than 1.1% (FEI Nova SEM, FEI Company, OR, USA; see Supporting information, Fig. S1). After calibration, the percentage errors of the AFM in the fast and slow scan direction were 0.98% and 0.20% respectively.

2.3 AFM imaging and analysis

Tissue samples were processed and imaged in air using a PicoPlus 5500 atomic force microscope (Agilent) in tapping mode as previously described [23, 24, 26]. Water and air comparison was carried out using a dimension icon AFM (Bruker AXS, Santa Barbara, CA, USA) in ScanAsyst fluid and air imaging modes. ScanAsyst fluid+ AFM probes (Bruker probes, nominal tip radius 2 nm, force constant 0.7 N/m) was used in both water and air imaging to reduce differences caused by different tip convolutions. Skin samples were imaged in deionized water and then dried by wicking away the water followed by exposure to a gentle stream of air for 30 min before re-imaging the same region in air. Following image capture, a rectangular region of interest was chosen along straight segments of individual fibrils (Fig. 1A). The selected regions spanned consistent topographical features (i.e. from gap region to gap region and through the middle of a given fibril). For each evaluated fibril, a two-dimensional fast fourier transform (2D-FFT) was performed using Scanning Probe Image Processor (SPIP; Image Metrology A/S, Hørsholm, Denmark) and the 2D power spectrum was analyzed to determine the value of the D-periodic spacing for that fibril.

BIOtec visions
www.biotecvisions.com

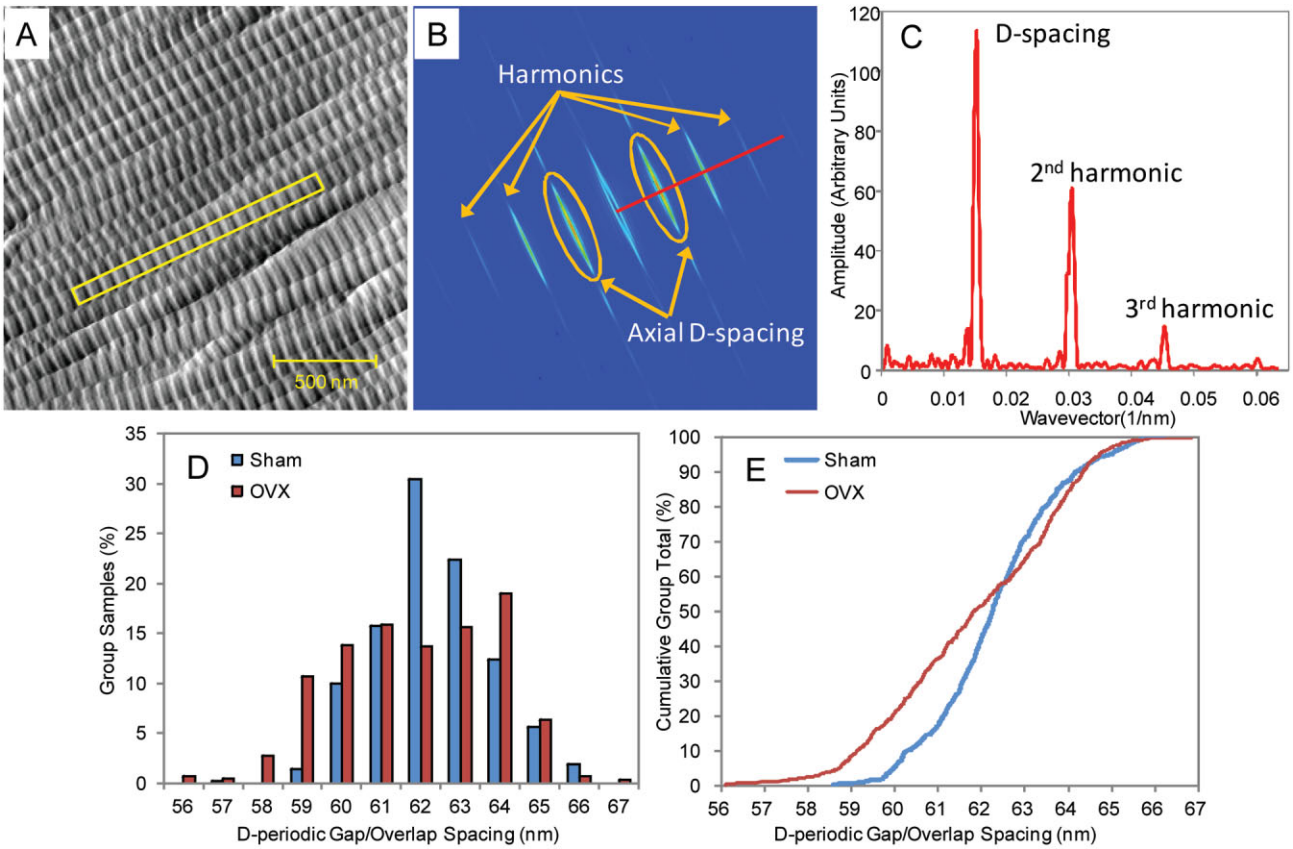

Figure 1. Schematic representation of the 2D-FFT process and D-periodic spacing measurements from sham-operated versus ovariectomized sheep dermis. (**A**) AFM amplitude image of type I collagen. The D-periodicity is visible as a striped pattern perpendicular to the fibril axis. (**B**) 2D-FFT of the selected fibril. The red line runs through the maximum value of the first peak, corresponding to the D-periodic spacing. (**C**) 1D-FFT along this line, normal to the D-periodic spacing and through the maxima in the 2D power spectrum. (**D**, **E**) Histogram and CDF representation of type I collagen D-periodic spacing distributions analyzed by 2D-FFT method. The comparison between sham-operated versus estrogen-depleted (OVX) sheep dermis was derived from previously published work [26]. In this case, there was a significant increase of diseased populations towards lower D-periodic spacings.

2.4 Computation

Model collagen fibrils were constructed in Matlab (The Mathworks, Nattic, MA, USA) as a summation of translated Gaussians. The power spectra of these model fibrils were computed and analyzed to determine the D-periodic spacing (the peak of the power spectrum) and D-periodic uncertainty [the standard deviation (SD) of the distribution of D-periodic spacing observed in the power spectrum]. The results were further analyzed and compared to results obtained from SPIP on real fibrils experimentally imaged using AFM.

2.5 Statistical analyses

To investigate differences in fibril morphology due to estrogen deficiency, D-periodic spacing values measured from an individual sample were averaged, yielding a single mean value for that sample, and then statistically compared using one-way ANOVA. Histograms were computed using a 1.0-nm bin size. To examine differences in the distribution of fibril morphologies between sham and OVX sheep, the cumulative distribution function (CDF) of each group was computed. The CDF shows what fraction of a given sample is contained up to a particular value, easily demonstrating differences between distributions in both mean and SD. To test for statistical significance between distributions, two-sample Kolmogorov-Smirnov (K-S) tests were then applied to the data sets.

3 Results and discussion

3.1 Aspects of measuring the D-periodic spacing in type I collagen fibrils

The axial D-periodic spacing was chosen as the key metric of collagen fibril morphology in this study. This measure captures aspects of collagen's fibrillar structure that may be related to the state of the individual molecular

Biotechnol. J. 2013, 8, 117–126

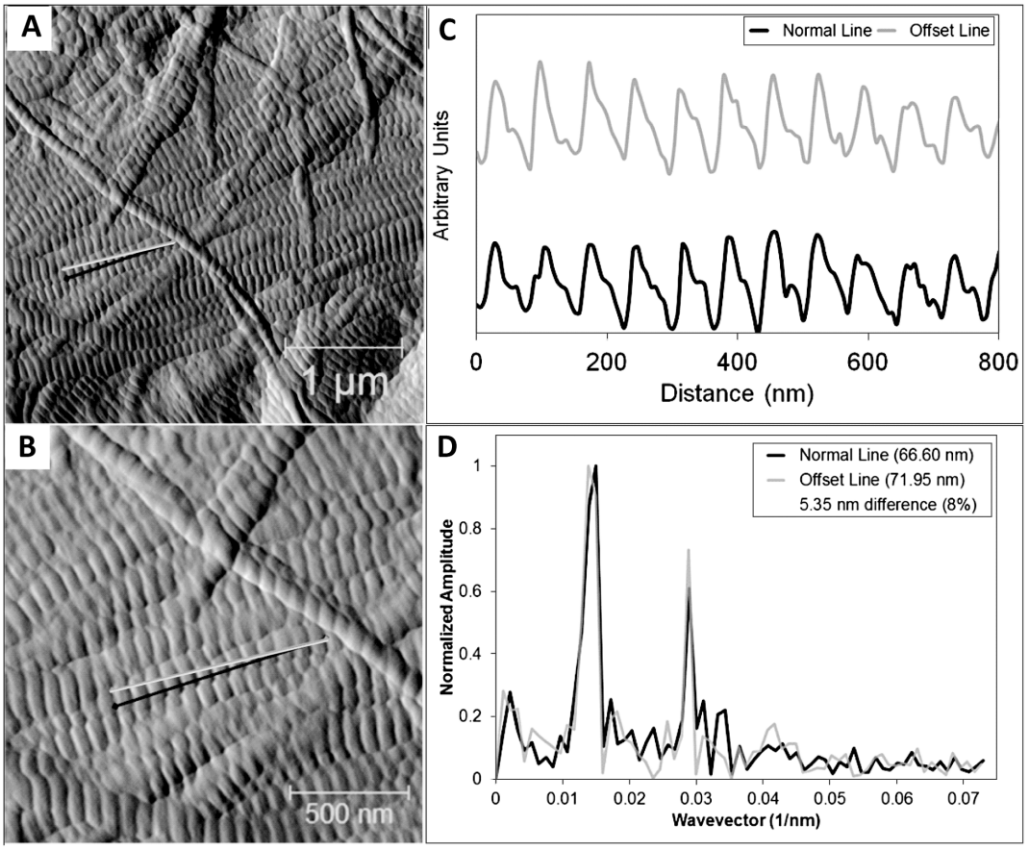

Figure 2. Effects of angle on 1D-FFT measurements of D-periodic spacing. This figure demonstrates the effect of changing the angle of the user-drawn line on the D-periodic spacing measurement derived using a 1D-FFT. (**A**) A 3.5 μm × 3.5 μm amplitude image showing a fibril chosen for analysis. (**B**) Enlargement of the analyzed area. The same fibril was measured using a line drawn normal to the D-periodic spacing (black) and one with a 5° tilt from normal (grey line). (**C**) Corresponding line scans from each line in **B**. (**D**) 1D-FFT derived from each line. In this example, there was a 5.4 nm difference in the measured D-periodic spacing (an 8% difference).

triple helices, post-translational modifications and/or cross-linking within the fibril. Although the functional mechanisms of these activities has not been elucidated, in many cases it has been shown that genetic modification, non-enzymatic cross-linking and other changes at the molecular level lead to significantly compromised bulk tissue properties [1]. As seen in Fig. 1A, D-periodic spacing is well resolved by AFM, providing a potential biomarker linked to the state of collagen. Previous studies have relied primarily on line scans and 1D-FFTs and did not perform quantitative analyses of larger data sets [29–32]. Line scans and 1D-FFTs suffer from two major limitations. First, lateral resolution is limited by a combination of factors including the pixel size of the image (~7 nm in images from the current study) and the radius of curvature of the probe (<10 nm). The periodic nature of the fibril can be exploited with a 1D-FFT to resolve the average spacing below the single-pixel limit, similar to the optical concept of super-resolution [33]. By fitting the FFT in reciprocal space to a continuous function, resolution can be achieved that is better than the limits set by pixel-related binning or apparent limits set by the radius of the probe. This interpolation scheme allows selection of the peak maximum with accuracy to tenths of a nanometer. An example calculation of this error using experimental data is included in Supporting information, Discussion #1.

The second and more significant limitation of line scans and 1D-FFTs is that they both rely on the user drawing a line along the length of a fibril, normal to the D-spacing [24]. From 1D-FFT measurements on fibrils in the current study, as little as a 5° deviation away from normal can alter the value measured for the spacing by as much as 8% (a difference of 5.4 nm on a 66.6 nm measurement, Fig. 2). Errors of this magnitude are larger than the population SDs noted below, masking important information within the distributions.

These types of error have provided a significant challenge to the observation of a distribution of D-period spacings in electron microscopy and AFM studies over the last seven decades. Employing a 2D-FFT approach decouples the determination of the D-periodic spacing from user bias in line location and angle selection. An example image of

a collagen fibril imaged by AFM and measured using a 2D-FFT approach is shown in Fig. 1. To minimize edge effects that can degrade resolution, a rectangular region of interest is drawn and extends from the edge of one gap zone to the edge of another gap zone, remaining within the width of the fibril. Figure 1B shows the 2D-FFT power spectrum from the selected region. The red line passes through the maximum value in the fundamental peak, therefore corresponding to the D-periodic spacing along the normal direction of the gap/overlap axis. A 1D-FFT along this line demonstrates that the D-periodic spacing, and the second and third harmonics are visible and well resolved (Fig. 1C).

The 2D-FFT analysis can be used to interpret D-spacing data from electron microscopy and AFM images. We have chosen AFM owing to its ability in keeping the tissue specimens relatively close to their native condition during sample preparation and imaging [34]. Absolute dehydration is thought to disrupt collagen molecular structure and increase packing density within a fibril [35, 36]. The effect of absolute dehydration has been shown to reduce collagen D-spacing [37, 38]. This implies hydration differences in the collagen fibrils could influence the observed distribution of collagen D-spacing. To demonstrate the effect of surface air-drying on collagen fibril D-spacing, we compared the metrical parameters of dermal collagen fibrils imaged by AFM in water and air. Dermis tissue was selected for this analysis because of the high water content in its native environment. As shown in the height images in Figs. 3A and B, the fibril surface imaged in water has greater height variation than the air-dried

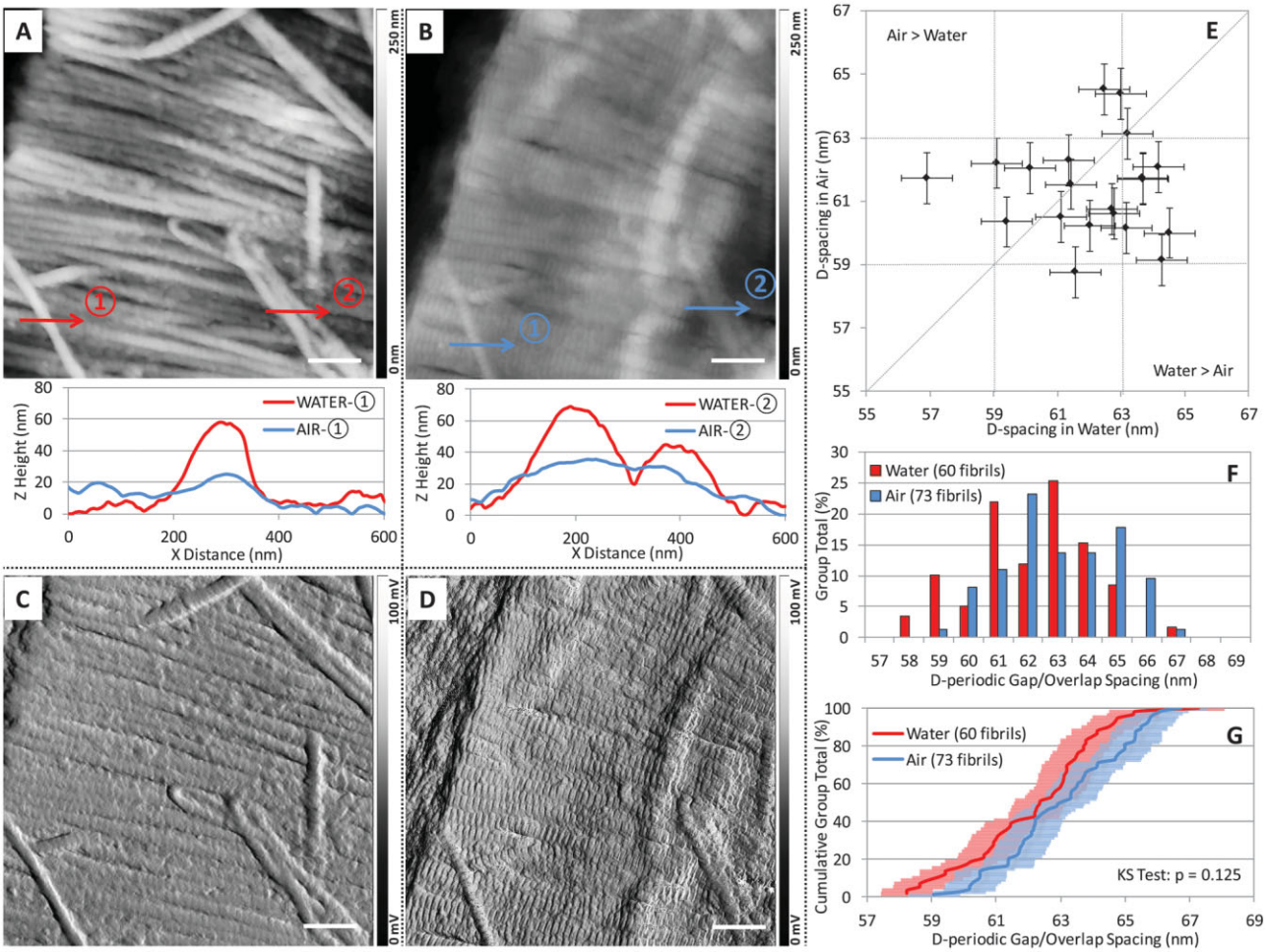

Figure 3. Comparison of sheep dermal collagen D-spacings measured in water and air. (**A**, **B**) Height images of sheep dermal collagen fibrils imaged in water and air respectively (both **A** and **B** are baseline subtracted using 2nd order polynominal fitting). Selected height profiles in the fast scan direction were plotted for the comparison of fibril heights in water and air (the local minimum was set as 0 nm in height). (**C**, **D**) Error images for regions **A** and **B**, respectively. D-spacings from a set of 20 fibrils were measured both in water and air error images. (**E**) The comparison is provided as a scatter plot. (**F**, **G**) Histogram and CDF representation of the water vs air fibril D-spacings measurement for an uncorrelated set of 133 fibrils. In this case, all the fibrils with discernible D-spacing repeat units from a set of seven images were included to generate the histogram in **F** and CDF in **G**. The error bars of 1.3 nm shown in **E** and **G** were derived from a combination of the absolute measurement error and the uncertainty of the 2D-FFT fibril spacing assessment. The scale bar is 500 nm in **A**–**D**.

surface. The height profiles illustrated by line scans (1) and (2) demonstrate an apparent swelling of the collagen fibrils, and possibly other matrix proteins such as proteoglycans, when imaged in water. Measurement of multiple fibrils indicated as much as a two- to four-fold increase in apparent fibril height in water relative to air. Error images shown in Figs. 3C and D demonstrate that fibril D-spacings can be directly observed in water and air, respectively. Using these images as well as six other sets, we were able to identify 20 fibrils with well-resolved D-spacing repeat units present in paired water and air images. Using 2D-FFT analysis, the D-spacings from the 20 fibrils were analyzed and are presented in the air vs water scatter plot (Fig. 3E). As illustrated in Fig. 3E, there was no correlation in the small shifts in D-spacings observed as a function of water vs air imaging. Indeed, 7 fibrils exhibited larger D-spacings in air and 11 exhibited larger D-spacings in water. Two fibrils were essentially unchanged. In addition to the direct comparison of individual fibril D-spacings, we also plotted the histogram and CDF including every fibril that was observed in either water (60 fibrils) or air imaging (73 fibrils) for the seven paired air/water images (Figs. 3F and G). The average fibril D-spacings in this analysis were 62.2 ± 2.0 nm and 63.1 ± 1.9 nm in water and air, respectively. The difference in absolute value of the average D-spacing (0.9 nm) for air vs water imaging obtained from Figs. 3E and F is of the same order as our ability to measure the spacings using the 2D-FFT method (see Supporting information, Fig. S3). The impact of air drying is small compared to the width of the D-spacing distribution as illustrated in Fig. 1 (discussed below). It is interesting to note that, although the histogram and CDF (Figs. 3F and G) indicate an average D-spacing increase of 0.9 nm upon air drying, the paired fibril data in Fig. 3E indicates that this average is obtained by a mix of behaviors ranging from 0 to 4 nm changes in D-spacing and both increases and decreases in D-spacing. This is also reflected in the substantial red/blue overlap, indicated in purple, in the CDF plot (Fig. 3G) and the p value of 0.125, indicating a lack of statistical significance. In summary, within the reproducibility of the measurement, there is no difference in D-banding spacing between the samples measured in air and water.

3.2 Analysis of D-periodic spacing measurements and associated uncertainties

The D-periodic spacing was modeled with a translated set of Gaussian functions, the amplitude and width of which were set by comparison to AFM images of type I collagen fibrils (Fig. 1A). The spacing between each gap was allowed to vary, and the sampling of the "numerical model fibril" was set to match experimental imaging conditions. The D-periodic spacing and its associated uncertainty were determined by fitting the FFT as shown in Supporting information, Fig. S2. To put an upper limit on the uncertainty associated with measurements from experimental samples, this 2D-FFT and fitting approach was also applied to collagen fibrils imaged in sheep bones (used as a control for a previously published experiment [24]). The D-periodic spacing was computed for fibrils from multiple locations within the bone using a maximum of 21 D-period repeat units (Supporting information, Table S1). The upper limit on the D-Period uncertainty, calculated as the mean of the SDs, was found to be 0.8 nm. This result sets the minimum bin size for histograms at 0.8 nm.

Sampling theory dictates that the uncertainty associated with the D-periodic spacing measurement should scale as the inverse of the number of repeat units, until the fundamental fibril variability is reached. The measured D-periodic spacing should also be independent of the sampling length scale (pixel size), provided the feature is well resolved. The results of varying both the sampling length along a model fibril, and the variability in D-periodic spacing within a fibril are show in Supporting information, Fig. S3. To achieve an SD of 0.8 nm or less, a minimum of nine D-period repeat units must be included in the 2D-FFT analysis. This figure ensures that the 2D-FFT method is insensitive to sampling length scales, given the 1/x dependence in both panels.

Making absolute x-y distance measurements with AFM and comparing absolute values measured in different studies has limitations. Absolute measurement relies on accurate calibration of AFM, which depends on the use of appropriate calibration standards, consistent performance of the piezo-material and regular calibration test to maintain the consistency. Due to the nonlinear relationship between scan size and scanner error, calibration over the range of D-spacing measurement (3.5 μm × 3.5 μm in the current study) using a feature size comparable to the collagen D-spacing (~67 nm) is critical. We calibrated the AFM using a 100 nm × 100 nm standard, and limited the scan error to 0.98% and 0.20% for x and y direction at 3.5 × 3.5 μm image size. For a fibril with 67 nm D-spacing, the absolute error in the AFM measurement is less than 1 nm. Note that the recommended calibration procedure of the AFM manufacturer utilizes a 10 μm × 10 μm calibration standard, which is 100 times larger than the collagen feature size. Non-linearities in the piezoelectric scanners introduce substantial error between these size scales, as detailed in the Supporting information, Discussion #2. Nevertheless, this calibration process only addresses the absolute calibration (accuracy) of the system. The calibration has no bearing on the differential sensitivity between measurements (precision), and does not limit one's ability to differentiate between population distributions measured using the same AFM with the same calibration parameters.

Thermal drift is another important issue to consider with any AFM imaging study. To investigate the impacts of thermal drift, a single 3.5 μm × 3.5 μm location was scanned up and down continuously over 1.5 h. Measure-

ments of the same individual fibrils within each image were then made and compared. This situation is an exaggeration of the thermal drift that may occur during normal scanning and even in this case, the drift on the fibril D-spacing measurement was less than 2 nm (Supporting information, Fig. S5). Over the time associated with taking one to two images for analysis at this size scale (less than 10 min), this drift is negligible. Nevertheless, to overcome this limitation and avoid problems that may originate from it, the vast majority of measured fibrils are selected to be within ± 45° from the fast scan axis. We have analyzed this issue previously [23] and the data are reproduced in the Supporting information, Fig. S6. Using data from normal bone samples, a data plot of D-periodic spacing as a function of the angle of the measured fibril was produced. If thermal drift in the slow scan direction was present in the data and leading to artifacts, bulges near –90° and 90° (along the slow axis) would exist. As this was not the case, the effects of thermal drift are not considered a major contributing factor in these measurements.

When using a surface-based technique such as AFM, the slope of the surface is another factor to consider. Hard samples (bone and dentin) are polished in an attempt to create a flat surface. However, to directly address sample slope, one can consider both experimental and theoretical approaches. In a previous study, collagen from the mouse tail tendon was directly adsorbed onto a mica surface [23]. Mica is often used as a substrate because it is atomistically flat, meaning that the observed topography is considered a characteristic of the sample and not of the substrate. In this case, a distribution of spacings was still observed and the mean spacing value was not statistically different from either bone or dentin samples, suggesting that slope in the bone and dentin samples was not responsible for the observed spacing distributions. Next, a theoretical surface was considered. Within a 30 μm × 30 μm image, 500 nm of tilt would equate to 0.96°. A tilt of this magnitude, if projected directly onto the long axis of a fibril, would cause a 67 nm spacing value to become 66.99 nm. Any such minor difference would be dwarfed by the spread of sample values. Increasing this tilt to 5 μm (almost 10° of tilt) would change the projected value to 66.1 nm. To directly address this concern in AFM images of bone specimens from a previous study [24], unflattened topography images were analyzed. Even with the largest tilt value observed in the 3.5 μm × 3.5 μm images (almost 9° of tilt), a spacing of 67 nm would become 66.2 nm. As demonstrated in previous publications using this technique [23, 24, 26, 28], this magnitude of tilt-induced difference cannot account for the large population shifts noted in cases of disease.

3.3 D-periodic spacing occurs with a distribution of values

This 2D-FFT approach was applied to type I collagen fibrils imaged within sham-operated sheep dermis using AFM (used as a control for a previously published experiment). The mean D-periodic spacing of the 624 measured fibrils was 62.3 nm, with a population SD of 1.4 nm. Figure 1D shows these data plotted as a histogram with a bin size of 1.0 nm (based on the maximum observed variation along a single fibril of 0.8 nm shown above). Note that the mean D-spacing value in dermal collagen has been reported to be less than 67 nm [39]. This histogram demonstrates that normal dermis contains fibrils with a distribution of D-periodic spacing values. A recent study demonstrated that this type of distribution also exists in other type I collagen-based tissues, including bone, dentin and tendon [23]. Based on these studies and other tissue samples measured to date [24, 26], the existence of a distribution of D-periodic spacings is a fundamental characteristic of type I collagen. However, the currently accepted models of type I collagen fibrillar structure completely overlook the presence of a distribution of spacing values [15]. For example, the possibility of a distribution was not discussed in a recent thorough book review of collagen structure and mechanics [1].

Previous studies have shown that D-spacing increases upon applying strain to a bone or tendon tissue [40–42]. Sasaki and coworkers [40] have shown that tendon D-spacing changes by 3% (~2 nm) at 20 MPa of stress; Puxkandl at al. [41] have shown a 1-nm change in tendon D-spacing at 3% macroscopic tissue strain; Gupta and Zioupos [42] reported 0.3-nm change in D-spacing at 1% tissue strain in bone. In addition to D-spacing elongation, interfibrillar sliding and shearing of proteoglycan-rich matrix are also thought to occur under conditions of tissue strain [41, 42]. The magnitude of D-spacing change as a function of applied strain is not large enough to explain the D-spacing distribution observed across multiple tissues, which has a typical range of 10 nm.

As a way to verify that this distribution is real and not caused by sample preparation or AFM imaging artifacts, the 2D-FFT analysis was performed on previously published SEM images from human Achilles tendons (Fig. 4, reproduced with permission from [12]). Qualitatively, the fibrils in Fig. 4A look similar to AFM images of collagen fibrils. Figure 4B shows the histogram results of the 2D-FFT analysis from 13 observed fibrils within the image (the included scale bar was used to set the length scale). The mean D-periodic spacing was 66.9 nm with a population SD of 1.6 nm. This mean value is well within the absolute experimental error of the AFM results. More importantly, a distribution of D-periodic spacings was observed in the SEM data.

To investigate a different non-surface-based method that has been used to analyze type I collagen nanoscale morphology, previously published small-angle X-ray scattering (SAXS) data from fresh, non-mineralized, turkey tendon samples were analyzed [27]. This analysis was performed to determine if the magnitude of distribution observed in D-period spacing is consistent with the ob-

Biotechnol. J. 2013, 8, 117–126

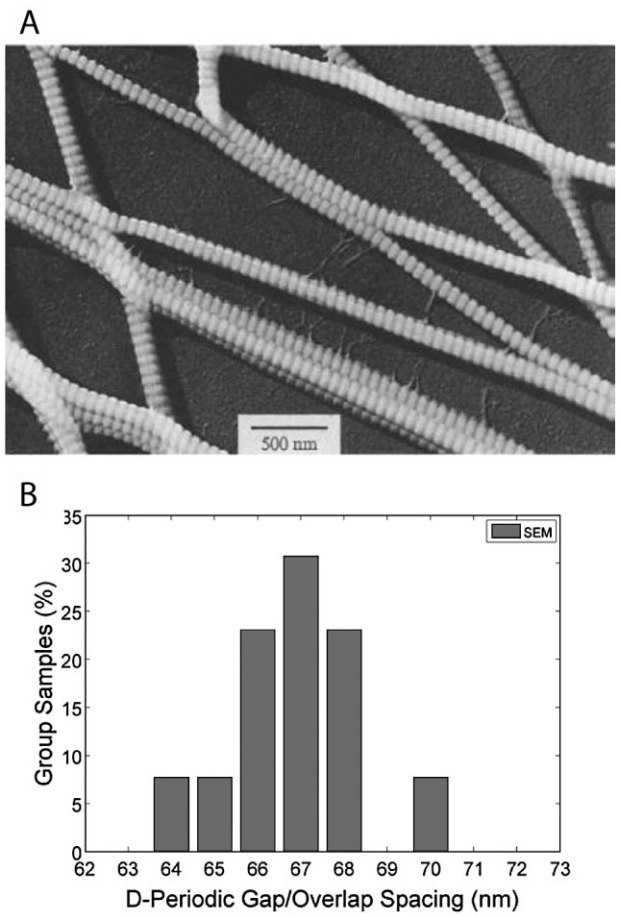

Figure 4. SEM image of type I collagen fibrils and histogram of D-periodic spacings. (**A**) SEM images of isolated type I collagen fibrils from Chapman et al. [12] (reproduced with permission from Elsevier). The D-periodic spacing of these fibrils was determined using the 2D-FFT technique described above. The internal reference bar set the length scale. (**B**) Distribution of D-periodic spacing values measured from 13 fibrils within the image. The distribution had a mean of 66.9 nm and an SD of 1.6 nm. The presence of a distribution of spacings corroborates that the existence of a distribution is a real feature and not an imaging artifact.

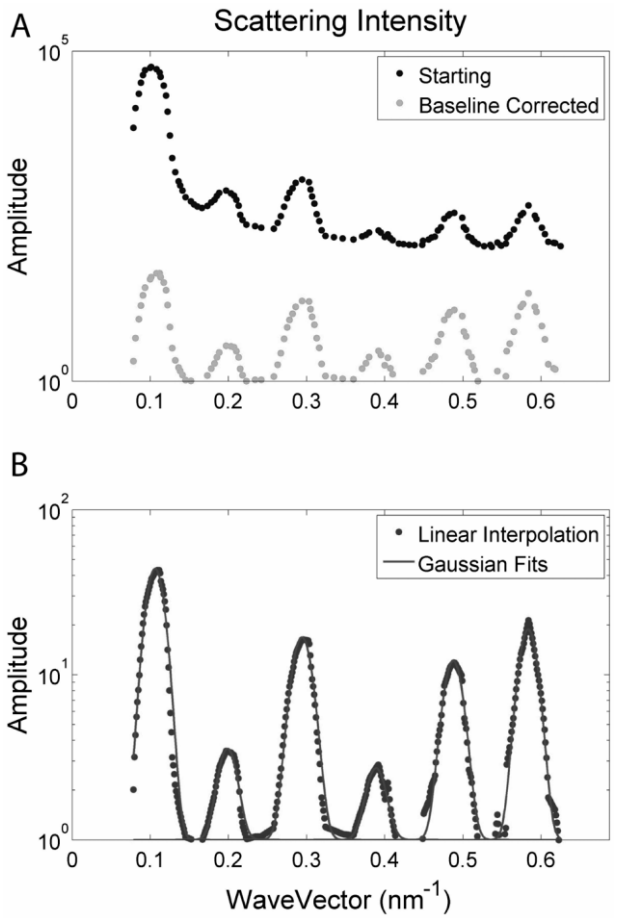

Figure 5. Analysis of SAXS scattering data from Fratzl et al. [28]. (**A**) The extracted intensities are shown as black dots. The grey dots show baseline corrected data fit to the following background form: $Y = Ax^{-B} + C$ where A = 1.1, B = -3.2, C = 10.9. (**B**) The dotted data are a linear interpolation of the grey data from (A), so that all data points are equally spaced. The solid lines are Gaussian fits to each scattering harmonic.

served peak widths from SAXS analyses of collagen. A modified Bertaut-Warren-Averbach (BWA) technique was used to determine what portion of the peak widths can be ascribed to the D-period spacing (Fig. 5) [43]. Full details of the analysis are provided as Supporting information, Discussion #3.

This analysis has two main findings. First, a D-period spacing distribution is sufficient to explain the observed peak width in the X-ray data. Second, the distribution width determined from the X-ray analysis was comparable to the distribution width observed using the 2D-FFT technique on individual fibrils. One significant advantage of the AFM 2D-FFT technique is that the fundamental resolution limit is sufficiently small to directly observe the shape of the sample distribution. The modified BWA technique cannot generate the sample distribution shape because the ability to fit the transformed data is insufficient to discriminate between different functional forms of an underlying distribution.

3.4 Statistical comparison of D-periodic spacing distributions as a function of disease

The existence of a distribution of D-periodic spacings is an important observation, standing in contrast to the fixed 67 nm value put forth 49 years ago. Utilizing an OVX model in sheep, which leads to estrogen depletion (an early model of osteoporosis), it was hypothesized that differences between normal skin and skin from animals with a known disease state could be detected through changes in collagen fibril morphology [25]. The mean D-periodic spacing of the sham population was 62.3 nm, not signifi-

cantly different from the 61.9 nm value in OVX samples ($p = 0.249$ using one-way ANOVA). When viewed as histograms (Fig. 1D), there was an observable increase in the OVX population towards lower D-periodic spacing values. Observing qualitative population differences between the normal and diseased states was an important finding, but proving statistical significance was imperative. Population differences were further highlighted when viewing the data as CDFs (Fig. 1E). The CDF plot from the sham population was then compared to that of the OVX population using a K-S test, chosen because it is a non-parametric comparison between distributions. This test is sensitive to changes in means as well as in the width of distributions, and does not require normally distributed data. The two-sample K-S test demonstrated a significant difference in the population distributions between sham and OVX samples ($p < 0.001$). These methods were also applied to a mouse model of human type IV OI, in which a known genetic mutation on collagen was created by substituting glycine with cysteine [26]. Similar to the estrogen-depletion model, no significant difference was noted in the means of D-spacing between the brittle mouse bones and wild-type bones. Significant differences were present in the population distributions of fibril spacings. We found 55% of brittle fibrils compared to 75% of wild-type fibrils within ± 1 SD (66–70 nm) range, which contributed to the statistically different CDF plots [26].

The origin of a D-spacing distribution and mechanisms of D-spacing changes that operate in diseases such as osteoporosis and OI are still unclear. We are currently pursuing these questions in our lab. Estrogen plays important roles in regulating metabolism, cell activities [44], and collagen turnover [45–47], etc. The change in D-spacing induced by estrogen depletion is a complex system to study. In OI, a point mutation results in the insertion of a bulkier residue in the molecular structure, which disrupts or destabilizes the triple helical conformation, through molecular kinking [48], free energy changes [49], weakening of intermolecular adhesion and reduction of cross-links [50]. These effects may lead to a change in D-spacing.

Although the mechanisms leading to these changes found in estrogen-deprived and OI tissues are still unclear, these studies provide evidence to show that collagen nanomorphology is altered, an important information that could potentially explain the compromised tissue properties, and be considered in disease diagnosis.

4 Concluding remarks

This paper details a systematic method to measure and analyze nanoscale characteristics of type I collagen fibrils using the D-periodic spacing as the key metric of nanoscale morphology. The ability to accurately measure the D-periodic spacing using a 2D-FFT approach led to the discovery of a distribution of type I collagen morphologies in four tissue types, bone, dentin, dermis and tendon. The importance of these observations was highlighted by demonstrating that statistically significant changes in population distributions could be observed in disease models of estrogen depletion and OI. The facts that distributions were present in both normal and diseased fibril populations, and that there were significant changes in these distributions with multiple diseases, have important implications for the structural model of type I collagen fibrils, and possibly to the diagnosis of type I collagen-based diseases. This type of analysis shows promise for providing important structural information regarding type I collagen in a wide variety of collagen-related ECM diseases and processes, such as photo aging, Ehlers-Danlos syndrome, OI, osteoporosis, wound healing, tissue engineering, and gene knockout model systems. Future work will be focused on the broader application of this method in ECM disease diagnosis and mechanistic studies. This method may find clinical uses in disease diagnosis and is already being employed for assessment of drug therapeutics.

We thank Judy Poore and Jeff Harrison at the Microscopy & Image Analysis Laboratory, University of Michigan, for technical services. This work was partially supported by the National Institute of Dental and Craniofacial Research (National Institutes of Health) through a Ruth L. Kirschstein National Service Award (Grant number 1F32DE018840-01 A1), the National Institutes of Arthritis and Musculoskeletal and Skin Diseases (Grant number AR50562), and a research grant from the Investigator Initiated Studies Program of Merck Sharp & Dohme Corp. The opinions expressed in this paper are those of the authors and do not necessarily represent those of Merck Sharp & Dohme Corp.

The authors declare no conflict of interest.

5 References

[1] Fratzl, P. (Ed.), *Collagen: Structure and Mechanics*, Springer, New York 2008.
[2] Kadler, K. E., Holmes, D. F., Trotter, J. A., Chapman, J. A., Collagen fibril formation. *Biochem. J.* 1996, *316*, 1–11.
[3] Kadler, K. E., Baldock, C., Bella, J., Boot-Hanford, R. P., Collagens at a glance. *J. Cell Sci.* 2007, *120*, 1955–1958.
[4] Canty, E. G., Kadler, K. E., Procollagen trafficking, processing and fibrillogenesis. *J. Cell Sci.* 2005, *118*, 1341–1353.
[5] Bear, R. S., Long x-ray diffraction spacing of collagen. *J. Am. Chem. Soc.* 1942, *64*, 727.
[6] Schmitt, F. O., Hall, C. E., Jakus, M. A., Electron microscope investigations of the structure of collagen. *J. Cell. Comp. Phys.* 1942, *20*, 11–33.
[7] Hodge, A. J., Petruska, J. A., Recent studies with the electron microscope on ordered aggregates of the tropocollagen molecule, in:

Ramachandran, G. N. (Ed.), *Aspects of Protein Structure*, Academic Press, New York 1963, p. 289.

[8] Bigi, A., Koch, M. H. J., Panzavolta, S., Roveri, N., Rubini, K., Structural aspects of the calcification process of lower vertebrate collagen. *Connect. Tissue Res.* 2000, *41*, 37–43.

[9] Fraser, R. D. B., MacRae, T. P., Miller, A., Suzuki, E., Molecular conformation and packing in collagen fibrils. *J. Mol. Biol.* 1983, *167*, 497–521.

[10] Eikenberry, E. F., Brodsky, B., Parry, D. A. D., Collagen fibril morphology in developing chick metatarsal tendons: I. X-ray diffraction studies. *Int. J.Biol. Macromol.* 1982, *4*, 322–328.

[11] Brodsky, B., Eikenberry, E. F., Characterization of fibrous forms of collagen. *Methods Enzymol.* 1982, *82 (Pt A)*, 127–174.

[12] Chapman, J. A., Tzaphlidou, M., Meek, K. M., Kadler, K. E., The collagen fibril – a model system for studying the staining and fixation of a protein. *Electron Microsc. Rev.* 1990, *3*, 143–182.

[13] Lin, A. C., Goh, M. C., Investigating the ultrastructure of fibrous long spacing collagen by parallel atomic force and transmission electron microscopy. *Proteins* 2002, *49*, 378–384.

[14] Arsenault, A. L., Image analysis of mineralized and non-mineralized type I collagen fibrils. *J. Electron Microsc. Tech.* 1991, *18*, 262–268.

[15] Orgel, J., Irving, T. C., Miller, A., Wess, T. J., Microfibrillar structure of type I collagen in situ. *Proc. Natl. Acad. Sci. USA* 2006, *103*, 9001–9005.

[16] Hulmes, D. J. S., Wess, T. J., Prockop, D. J., Fratzl, P., Radial packing, order, and disorder in collagen fibrils. *Biophys. J.* 1995, *68*, 1661–1670.

[17] Hulmes, D. J. S., Miller, A., Quasi-hexagonal molecular packing in collagen fibrils. *Nature* 1979, *282*, 878–880.

[18] Fraser, R. D. B., MacRae, T. P., Miller, A., Molecular packing in type I collagen fibrils. *J. Mol. Biol.* 1987, *193*, 115–125.

[19] Orgel, J. P. R. O., Miller, A., Irving, T. C., Fischetti, R. F. et al., The in situ supermolecular structure of type I collagen. *Structure* 2001, *9*, 1061–1069.

[20] Trus, B. L., Piez, K. A., Compressed microfibril models of the native collagen fibril. *Nature* 1980, *286*, 300–301.

[21] Piez, K. A., Trus, B. L., A new model for packing of type-I collagen molecules in the native fibril. *Biosci. Rep.* 1981, *1*, 801–810.

[22] Gautieri, A., Vesentini, S., Redaelli, A., Buehler, M. J., Hierarchical structure and nanomechanics of collagen microfibrils from the atomistic scale up. *Nano Lett.* 2011, *11*, 757–766.

[23] Wallace, J. M., Chen, Q., Fang, M., Erickson, B. et al., Type I collagen exists as a distribution of nanoscale morphologies in teeth, bones, and tendons. *Langmuir* 2010, *26*, 7349–7354.

[24] Wallace, J. M., Erickson, B., Les, C. M., Orr, B. G., Banaszak Holl, M. M., Distribution of type I collagen morphologies in bone: Relation to estrogen depletion in bone. *Bone* 2010, *46*, 1349–1354.

[25] Fang, M., Liroff, K. G., Turner, A. S., Les, C. M. et al., Estrogen depletion results in nanoscale morphology changes in dermal collagen. *J. Invest. Dermatol.* 2012, *132*, 1791–1797.

[26] Wallace, J. M., Orr, B. G., Marini, J. C., Banaszak Holl, M. M., Nanoscale morphology of type I collagen is altered in the Brtl mouse model of osteogenesis imperfecta. *J. Struct. Biology* 2011, *173*, 146–152.

[27] Fratzl, P., Fratzlzelman, N., Klaushofer, K., Collagen packing and mineralization – an X-ray-scattering investigation of turkey leg tendon. *Biophys. J.* 1993, *64*, 260–266.

[28] Fang, M., Liroff, G. K., Turner, A. S., Les, C. M. et al., Estrogen Depletion results in nanoscale morphology changes in dermal collagen *J. Invest. Dermatol.* 2012, *132*, 1791–1797.

[29] Habelitz, S., Balooch, M., Marshall, S. J., Balooch, G., Marshall, G. W., In situ atomic force microscopy of partially demineralized human dentin collagen fibrils. *J. Struct. Biol.* 2002, *138*, 227–236.

[30] Hassenkam, T., Fantner, G. E., Cutroni, J. A., Weaver, J. C. et al., High-resolution AFM imaging of intact and fractured trabecular bone. *Bone* 2004, *35*, 4–10.

[31] Baranauskas, V., Garavello-Freitas, I., Jingguo, Z., Cruz-Hofling, M. A., Observation of the bone matrix structure of intact and regenerative zones of tibias by atomic force microscopy. *J. Vacuum Sci. Technol. A* 2001, *19*, 1042–1045.

[32] Kindt, J. H., Thurner, P. J., Lauer, M. E., Bosma, B. L. et al., In situ observation of fluoride-ion-induced hydroxyapatite-collagen detachment on bone fracture surfaces by atomic force microscopy. *Nanotechnology* 2007, *18,* 135102.

[33] Cremer, C., Kaufman, R., Gunkel, M., Pres, S. et al., Superresolution imaging of biological nanostructures by spectral precision distance microscopy. *Biotechnol. J.* 2011, *6*, 1037–1051.

[34] Wallace, J. M., Applications of atomic force microscopy for the assessment of nanoscale morphological and mechanical properties of bone. *Bone* 2012, *50*, 420–427.

[35] Buehler, M. J., Keten, S., Ackbarow, T., Theoretical and computational hierarchical nanomechanics of protein materials: Deformation and fracture. *Prog. Mater. Sci.* 2008, *53*, 1101–1241.

[36] Mogilner, I. G., Ruderman, G., Grigera, J. R., Collagen stability, hydration and native state. *J. Mol. Graphics Model.* 2002, *21*, 209–213.

[37] Price, R. I., Lees, S., Kirschner, D. A., X-ray diffraction analysis of tendon collagen at ambient and cryogenic temperatures: Role of hydration. *Int. J.Biol. Macromol.* 1997, *20*, 23–33.

[38] Habelitz, S., Balooch, M., Marshall, S. J., Balooch, G., Marshall G. W. Jr., In situ atomic force microscopy of partially demineralized human dentin collagen fibrils. *J. Struct. Biol.* 2002, *138*, 227–236.

[39] Brodsky, B., Eikenberry, E. F., Cassidy, K., An unusual collagen periodicity in skin. *Biochim. Biophys. Acta* 1980, *621*, 162–166.

[40] Sasaki, N., Shukunami, N., Matsushima, N., Izumi, Y., Time-resolved X-ray diffraction from tendon collagen during creep using synchrotron radiation. *J. Biomech.* 1999, *32*, 285–292.

[41] Puxkandl, R., Zizak, I., Paris, O., Keckes, J. et al., Viscoelastic properties of collagen: Synchrotron radiation investigations and structural model. *Philos. Trans. R. Soc. B Biol.Sci.* 2002, *357*, 191–197.

[42] Gupta, H. S., Zioupos, P., Fracture of bone tissue: The 'hows' and the 'whys'. *Med. Eng. Phys.* 2008, *30*, 1209–1226.

[43] Drits, V. A., Eberl, D. D., Srodon, J., XRD measurement of mean thickness, thickness distribution and strain for illite and illite-smectite crystallites by the Bertaut-Warren-Averbach technique. *Clays Clay Miner.* 1998, *46*, 38–50.

[44] Haczynski, J., Tarkowski, R., Jarzabek, K., Slomczynska, M. et al., Human cultured skin fibroblasts express estrogen receptor alpha and beta. *Int. J. Mol. Med.* 2002, *10*, 149–153.

[45] Dimitrios J, H., Ioannis I, A., Bone remodeling. *Ann. N. Y. Acad. Sci.* 2006, *1092*, 385–396.

[46] Brincat, M. P., Baron, Y. M., Galea, R., Estrogens and the skin. *Climacteric* 2005, *8*, 110–123.

[47] Brincat, M., Moniz, C. J., Studd, J. W. W., Long-term effects of the menopause and sex hormones on skin thickness. *Br. J. Obstet. Gynaecol.* 1985, *92*, 256–259.

[48] Chang, S.-W., Shefelbine, S. J., Buehler, M. J., Structural and mechanical differences between collagen homo- and heterotrimers: Relevance for the molecular origin of brittle bone disease. *Biophys. J.* 2012, *102*, 640–648.

[49] Lee, K. H., Kuczera, K., Banaszak Holl, M. M., The severity of osteogenesis imperfecta: A comparison to the relative free energy differences of collagen model peptides. *Biopolymers* 2011, *95*, 182–193.

[50] Gautieri, A., Uzel, S., Vesentini, S., Redaelli, A., Buehler, M. J., Molecular and mesoscale mechanisms of osteogenesis imperfecta disease in collagen fibrils. *Biophys. J.* 2009, *97*, 857–865.